Published in final edited form as:

RSC Adv. 2012 March 7; 2(5): 1970–1978. doi:10.1039/C2RA00857B.

A potential nanobiotechnology platform based on infectious bursal disease subviral particles

Omid Taghavian[a], **Manoj K. Mandal**[a], **Nicole F. Steinmetz**[b], **Stefan Rasche**[a], **Holger Spiegel**[a], **Rainer Fischer**[a,c], and **Stefan Schillberg**[a,*]

[a]Fraunhofer IME, Forckenbeckstraβe 6, 52074, Aachen, Germany

[b]Department of Biomedical Engineering, School of Medicine, Case Western Reserve University, 10900 Euclid Ave., Cleveland, OH 44106, USA

[c]Institut für Molekulare Biotechnologie, RWTH Aachen University, Worringerweg 1, 52074, Aachen, Germany

Abstract

We describe a novel nanobiotechnology platform based on subviral particles derived from *infectious bursal disease virus* (IBD-SVPs). The major virus coat protein VP2 assembles into spherical, 23 nm SVPs when expressed as a heterologous protein in the yeast *Pichia pastoris*. We recovered up to 38 mg of IBD-SVPs at > 95% purity from 1 L of recombinant yeast culture. The purified particles were able to tolerate organic solvents up to 20% concentration (ethanol or dimethylsulfoxide), they resisted temperatures up to 65 °C and remained stable over a wide pH range (2.5–9.0). We achieved bioconjugation to the amine groups of lysine residues and to the carboxyl groups of aspartic and glutamic acid residues, allowing the functionalization of IBD-SVPs with biotin. The accessibility of surface amine groups was measured using Alexa Fluor 488 *N*-hydroxysuccinimide (NHS) ester, an amine-selective fluorescent dye, revealing that approximately 60 dye molecules were attached to the surface of each particle. IBD-SVPs can therefore be exploited as a robust and versatile nanoscaffold to display diverse functional ligands.

Graphical Abstract

We investigated the stability of yeast-derived infectious bursal disease subviral particles (IBD-SVPs) against heat, pH and organic solvents, and as a potential novel nano-carrier for biotin and fluorescent dye residues.

stefan.schillberg@ime.fraunhofer.de; Fax: +49-241-6085-10000; Tel: +49-241-6085-11050.

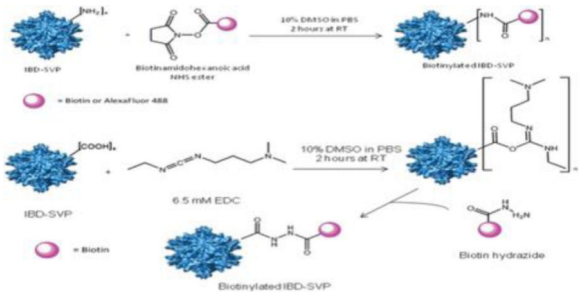

Introduction

Viral nanoparticles (VNPs) are nanoscale devices based on natural viruses.[1–5] They offer advantages over synthetic nanoparticles such as carbon nanotubes and quantum dots[6] because they are biocompatible, biodegradable and non-toxic. They provide a robust and symmetrical structure, amenable to both genetic and chemical modifications[7] for the development of novel nanoscale formulations, and can be used for example as nanotemplates, nanoprobes and nanoreactors.[8] Importantly, VNPs are stable, symmetrical, monodisperse particles with a distinct size, atomic precision and uniform multivalency; they are also easy to prepare in large quantities.[9] VNPs derived from mammalian viruses are already widely used, but concerns about their potential toxicity and pathogenicity have led to the more recent development of plant VNPs,[1,10,11] which are safer and can be prepared in gram quantities from a few kilograms of infected leaves.[2,12,13] Spherical VNPs based on *Cowpea mosaic virus* (CPMV),[14–18] *Cowpea chlorotic mottle virus* (CCMV)[19] and *Turnip yellow mosaic virus* (TYMV),[20] as well as rod-shaped VNPs based on *Tobacco mosaic virus* (TMV),[21] have been investigated for this purpose. The majority of research has focused on CPMV making this virus the gold standard for stability, addressability and functionalization.[22–25]

As an alternative to VNPs, virus coat proteins (CPs) can be expressed in recombinant yeast cells to produce nanoparticles in higher amount that lack the virus genome, thus providing further safety.[26,27] Some viral coat proteins assemble spontaneously either into virus-like particles (VLPs), which have the same size and morphology as the parent virus, or into subviral particles (SVPs), which differ from the parent virus in size and structure often because the parent virus comprises several different CP subunits whereas SVPs are homomeric.[28–32]

The absence of genomic nucleic acid leaves spaces for the encapsidation of small useful molecules, *e.g.* drugs, imaging reagents or nucleic acids.[33,34] Furthermore, the structure of the particles can be modified by genetic engineering *e.g.* to present antigens,[14,27,35] to make the surface more favorable for the nucleation of a specific mineral or alloy,[4,36,37] or to introduce one or more amino acids modified to display a specific chemical group for structural stabilization or conjugation.[38–40] Modification also provides an opportunity to optimize the physicochemical properties of the particle, which must be tailored for specific applications. For example, nanoparticles designed as contrast agents for magnetic resonance imaging (MRI) should encourage mineralization whereas those used for electronics

applications need to be stable in acid, ethanol and at high temperatures. VNPs used for biomedical applications such as imaging or drug delivery often need to be bioconjugated in the presence of dimethylsulfoxide (DMSO), so the particles must be stable in this organic solvent.[5]

Infectious bursal disease virus (IBDV, *Birnaviridae*) is a double-stranded RNA virus comprising a non-enveloped icosahedral capsid with a T = 13 surface lattice, which causes a contagious form of immunosuppression in young chickens.[41] We expressed the major IBDV coat protein (VP2) in *Pichia pastoris* to investigate the physical stability and chemical addressability of infectious bursal disease subviral particles (IBD-SVPs). Doughnut-like icosahedral particles, 23 nm in diameter and with a T = 1 surface lattice were produced as previously described.[34,42–44] The particles displayed solvent exposed functional sites suitable for chemical modification, such as the amine groups of five lysine residues (Lys 81, 192, 309, 316 and 381) and the carboxylic groups of four glutamic acid residues (Glu 300, 311, 355 and 378) and nine aspartic acid residues (Asp 51, 83, 138, 190, 213, 267, 279, 287 and 323) per coat protein (Fig. 1). We tested traditional bioconjugation methods using the addressable lysine, aspartic acid and glutamic acid side chains[45] and achieved the bioconjugation of biotin to amine groups on exposed lysine side chains and to carboxyl groups on aspartic and glutamic acid residues. These biotinylated residues may provide attachment sites for other molecules such as streptavidin-conjugated peptides, enzymes, antibodies, gold particles and fluorescent dyes, allowing the functionalization of IBD-SVPs with multiple functional ligands.

Experimental

Plasmid construction and transformation The *VP2* cDNA for expression in yeast was amplified by PCR from strain IR01[46] using the primers VP2-forward (5′-CGC G_A_A_ T_T_C_ ACA ACA CAA ATC AGA TTT ATA GAG AGA TTT ATA AAA AAA AAA AAC-3′) and VP2-reverse (5′-GCT_ C_T_A_ G_A_T TTA GTG ATG GTG ATG GTG ATG TGC TCC TGC AAT CTT CAG-3′). The product was transferred to expression vector pPICZ B (Invitrogen, Karlsruhe, Germany) using the *Eco*RI and *Xba*I restriction sites (underlined) where it was placed under the control of the methanol-inducible alcohol oxidase (*AOX1*) promoter. The recombinant vector was introduced into *Pichia pastoris* strain X-33 (Invitrogen) as previously described.[47]

VP2 expression, and SVP extraction and purification

Recombinant yeast cells were cultured in YPD medium (1% (w/v) yeast extract, 2% (w/v) peptone, 2% (w/v) dextrose) as recommended (EasySelect™ *Pichia* Expression Kit, Invitrogen). VP2 expression was induced by resuspending cells to a final cell density of OD_{600} = 1.0 in BMMY medium (100 mM sodium phosphate pH 6.0, 1% (w/v) yeast extract, 2% (w/v) peptone, 1.34% (w/v) yeast nitrogen base, 0.4 μg ml^{-1} biotin) containing 0.5% (v/v) methanol. The most productive cells were identified by immunoblotting, and were cultured in 500 ml BMMY medium for 4 d as recommended (Invitrogen). Methanol was added to a final concentration of 0.5% (v/v) on the second day, increasing to 1% (v/v) on the third day. The cells were then harvested by centrifugation at 3000 × g for 5 min, resuspended

in breaking buffer (100 mM sodium acetate pH 4.0, 1 mM PMSF, 1 mM EDTA, 5% (v/v) glycerol) and disrupted by five passes in a microfluidizer (Newton, MA, USA). The supernatant was collected after centrifugation at 13 000 × g for 30 min and the SVPs were precipitated by 50% ammonium sulfate and resuspended in 5 ml phosphate-buffered saline (PBS). The extract was purified by size exclusion chromatography (SEC) on a Hiprep 26/60 Sephacryl S400 HR column (GE HealthCare, Freiburg, Germany) and the SVP elution fractions were concentrated using a Vivaspin 20 spin column with a 300 kDa cut-off membrane (Sartorius-Stedim, Göttingen, Germany). The purity of the IBD-SVPs was determined by densitometric analysis of gels stained with Coomassie Brilliant Blue, using AIDA image analysis software.

Testing SVP stability

The solvent stability of the SVPs was tested by dissolving purified particles in 5, 10, 20 or 50% (v/v) ethanol–water or DMSO–water to a final concentration of 1 mg ml^{-1}, with SVPs diluted to the same concentration in PBS as a control. All samples were incubated at room temperature for 24 h then centrifuged at 13 000 × g for 20 min prior to analysis. To test temperature stability, 50 μl aliquots of purified SVPs (1 mg ml^{-1}) were incubated at 25, 40, 50, 60, 65, 68.5, 72, 75, 80 and 90 °C for 1 h prior to centrifugation as above. To test pH stability, purified SVPs were dissolved in 50 mM acetate buffer pH 2.5, 50 mM acetate buffer pH 5.5, PBS pH 7.4, 50 mM Tris-HCl pH 8.0 or 50 mM Tris-HCl pH 9.0, to a final concentration of 0.5 mg ml^{-1}. After overnight incubation at room temperature, the samples were centrifuged as above. In all three cases, the stability, conformation and integrity of the SVPs were determined by NAGE, spectroscopy, DLS and TEM as described below.

Native agarose gel electrophoresis (NAGE)

VP2 samples were separated by 1% (w/v) native agarose gel electrophoresis at 50 V for 1 h. The agarose gel was prepared in buffer A (25 mM Tris-HCl pH 8.15, 19.2 mM glycine) as previously described.[48] The protein bands were visualized by staining with Coomassie Brilliant Blue.

Spectroscopy

After solvent exposure, temperature and pH testing, each VP2 sample was centrifuged at 13 000 × g for 20 min, and the absorbance spectrum (UV/Vis, 220–310 nm) was measured using a nanodrop spectrophotometer (PeQlab Ltd., Erlangen, Germany). The total quantity of soluble protein was estimated from the A280 value (mean from three replicates). After dyemolecule coupling, the absorbance was measured using the “protein and labels” option on the spectrophotometer.

Dynamic light scattering (DLS)

The radius of SVPs in solution (0.5 ml aliquots, 1 mg ml^{-1}) was determined by DLS in self-beating mode on an ALV set-up comprising a 473 nm solid-state laser (Koheras, Kleinostheim, Germany) operating at a 60° angle. Experimentally measured autocorrelation functions (ACFs) of the intensity fluctuations g(2)(t) were determined using the CONTIN algorithm,[49,50] yielding the distribution of the relaxation time *t*.

Immunogold staining and transmission electron microscopy (TEM)

The morphology of the particles was investigated by applying 30 μl aliquots of each sample onto discharged, 400 mesh carbon-coated nickel grids (Plano, Wetzlar, Germany) for 15 min. Excess particles were removed by rinsing with PBS. For conjugation analysis, the grids were blocked with 1% (w/v) BSA containing 0.1% (w/v) sodium azide for 30 min. Goat *anti*-biotin (1 : 20 in PBS) antibodies labeled with 6 nm gold particles (Aurion, Wageningen, The Netherlands) were used for detection. The grids were incubated for 1 h with the antibody and washed three times each with PBS containing 0.5% (v/v) Tween-20 (PBST) then distilled water. Finally, the grids were negatively stained with a 2% (w/v) aqueous uranyl acetate and observed under a 400T electron microscope (Philips, Eindhoven, the Netherlands) operated at 60 kV accelerating voltage. Digital images were captured with an Olympus camera (MORADA) and processed using iTEM software (Münster, Germany).

Chemical bioconjugation

Biotin was conjugated to the amine group of lysine residues or the carboxyl group of aspartic and glutamic acid residues exposed to the solvent.[44] As shown in Fig. 1, IBD-SVPs display five lysine residues (Lys 81, 192, 309, 316 and 381), four glutamic acid residues (Glu 300, 311, 355 and 378) and nine aspartic acid residues (Asp 51, 83, 138, 190, 213, 267, 279, 287 and 323) per coat protein; IBD-SVPs are formed by 60 copies of identical coat protein units. Alexa Fluor 488 *N*-hydroxysuccinimide (NHS) ester and the DyLight™ antibody labeling kit (Pierce, Bonn, Germany) were used to determine the number of accessible amines.

Conjugation to amine groups was achieved using 1 mg ml^{-1} SVPs and biotinamidohexanoic acid NHS ester (Sigma, Deisenhofen, Germany) dissolved in DMSO to a concentration of 2.1 mM, and mixed with PBS to a final DMSO concentration of 10% (v/v). The ratio of biotin to IBD-SVP was 6000 : 1. The reaction was allowed to proceed for 2 h at 4 °C with gentle agitation.

Conjugation to carboxyl groups was achieved by dialyzing SVPs in PBS against 0.1 M MES buffer (pH 5.5) using a Nanosep centrifugal device with a 100 kDa MWCO (Pall, Dreieich, Germany). SVPs in MES buffer at a final concentration of 0.5–3.5 mg ml^{-1} were incubated with 6.5 mM EDC (1-[3-(dimethylamino)propyl]-3-ethylcarbodiimide methiodide) and 2 mM biotin hydrazide in DMSO (Sigma). The biotin hydrazide was used at a molar excess of 7800–15 600 : 1 biotin : IBD-SVP and the final DMSO concentration was 10% (v/v). The reaction was allowed to proceed overnight at room temperature with gentle agitation to prevent precipitation.

Modified particles were purified on a Hiprep 26/60 Sephacryl S400 HR column (GE HealthCare) and the SVP peak was concentrated using a Vivaspin 20 with 300 kDa cut-off membrane (Sartorious).

Western blot analysis

To confirm successful biotinylation, 10–20 μg of biotin-labeled SVPs were loaded on a 12% (w/v) SDS-polyacrylamide gel for separation, then transferred onto a nitrocellulose

membrane and blocked in 5% (w/v) skimmed milk in PBS containing 0.01% (v/v) Tween 20 (PBST). Particles were detected either by subsequent incubation with rabbit *anti*-IBD-VP2 (1 : 10 000) and phosphatase-conjugated goat *anti*-rabbit antibody (final concentration 2 μg ml^{-1}) each for 1 h or by incubating with alkaline phosphatase-conjugated streptavidin (final concentration 0.2 μg ml^{-1} in PBS) for 1 h at room temperature, with gentle agitation. After three 20 min washes with PBST, the signal was detected with NBT/BCIP (Sigma).

Results

Recovery and yield of heterologous SVPs

We were able to recover 38 mg of > 95% pure IBD-SVPs from 1 L of the *Pichia pastoris* cell extract after downstream processing by pH shifting, ammonium sulfate precipitation and SEC. We then determined particle stability in different solvents, at different temperatures and in different pH-buffered solutions by measuring the soluble protein content at A280, determining electrophoretic mobility under native conditions, and studying particle conformation and morphology by DLS and TEM.

Solvent stability

The stability of nanoparticles in solvents is an important requirement because bioconjugation is usually carried out in an environment containing up to 20% (v/v) DMSO, whereas mineralization (*e.g.* with silica) requires up to 20% (v/v) ethanol as a solvent. We therefore dissolved the SVPs in ethanol–water and DMSO–water solutions, with PBS as a control.

The electrophoretic mobility of SVPs under native conditions is shown in Fig. 2A. Particles prepared in up to 20% (v/v) solutions of either ethanol or DMSO exhibited the same mobility as those prepared in PBS. SVP solubility decreased gradually as the ethanol concentration increased from 5 to 20% (v/v) (Fig. 2A,B) and complete precipitation occurred in a 50% (v/v) solution. In contrast, there was little change in SVP solubility as the DMSO concentration increased to 20% (v/v), and only partial precipitation occurred at 50% (v/v) along with an increase in electrophoretic mobility (Fig. 2A,B). Although the particles were stable in up to 20% (v/v) of DMSO, amine and carboxylate coupling worked also using a 10% (v/v) solution (data not shown).

Conformational changes in the particles were monitored by DLS, reflecting changes in the mean particle hydrodynamic radius. We observed two peaks, the first (~12 nm) corresponding to the hydrodynamic radius of single intact particles and the second (~100 nm) corresponding to particle aggregates (Fig. 2C). Increasing the ethanol concentration to 20% (v/v) appeared to have no impact on conformation, most of the particles still gathering in the first peak. In contrast, some aggregation was apparent at 20% (v/v) DMSO because the particles were distributed evenly between the two peaks (Fig. 2C). At 50% (v/v) DMSO, there was a significant shift towards the second peak as most of the particles aggregated. TEM analysis confirmed the changing conformation of particles at high solvent concentrations (Fig. 2D). These results show that IBD-SVPs can tolerate up to 20% (v/v)

ethanol or 20% (v/v) DMSO, confirming their suitability for bioconjugation and mineralization reactions under standard conditions.

Temperature stability

The electrophoretic mobility of the IBD-SVPs under native conditions remained constant after incubation for 1 h at temperatures between 25 and 60 °C (Fig. 3A). No precipitation or conformational changes were observed within this temperature range (Fig. 3B,C,D). This indicates that IBD-SVPs are relatively heat resistant, with temperature stability comparable to that of CPMV particles.[51] At temperatures above 60 °C, extensive precipitation was observed along with significant changes in electrophoretic mobility and conformation (Fig. 3A–D).

Stability in different pH environments

SVP preparations were dispersed in buffer solutions with pH values of 2.5, 5.5, 8.0 and 9.0. PBS (pH 7.4) was used as the reference buffer. The SVPs remained stable after incubation in these buffers at room temperature for 24 h. The electrophoretic mobility of the SVPs was similar over the pH range 5.5–9.0, but increased slightly at pH 2.5 probably reflecting changes to the net charge on the particle surface (Fig. 4A). There was no significant difference in particle solubility over the pH range 2.5–9.0, suggesting there was no aggregation or precipitation (Fig. 4B) and in agreement there was no significant shift in the particle hydrodynamic radius (Fig. 4C). TEM revealed slight conformational change at pH 5.5 and pH 9.0 but this did not affect the particle radius (Fig. 4D).

Addressability of IBD-SVPs

VP2 contains two cysteine residues that do not participate in disulfide bond formation, but the side chains are not exposed to the solvent and are therefore poor targets for bioconjugation (Fig. 1C). However five lysine residues present accessible amine groups (Lys 81, 192, 309, 316 and 381) and there are 13 acidic residues that present accessible carboxyl groups (Asp 300, 311, 355, 378 and Glu 51, 83, 138, 190, 213, 267, 279, 287 and 323). Each SVP comprises 60 VP2 monomers, resulting in a total of 300 potentially addressable amines and 780 carboxyl groups per particle. We also attempted to glycosylate the IBD-SVPs by targeting VP2 for secretion since the protein has three potential glycan acceptor sites, but the glycosylated monomers were unable to assemble into SVPs (data not shown).

Addressability of amine groups

We determined the number of addressable amines on each SVP by coupling DyLight 488 NHS ester to the particles using the DyLight™ Antibody Labeling Kit (Pierce). We used 1 mg of IBD-SVPs (2 mg ml^{-1}) per dye batch and the dye concentration (c) was determined by measuring its absorbance (A) at 493 nm and using the dye-specific molar extinction coefficient (ε) of 70 000 (A = cdε, with d = pathlength). This showed that on average 63 dye molecules were attached to each particle.

We also used biotinamidohexanoic acid NHS ester to determine whether biotin could be installed on the accessible amine groups. The reaction was carried out at pH 7.4 because under these conditions only the amine groups of lysine residues exposed to the solvent are

expected to react with the ester (Fig. 5). The coupling of biotin to the SVPs was confirmed by western blot using alkaline phosphatase-conjugated streptavidin (Fig. 6A). SEC showed that the particle mass had increased after biotinylation (Fig. 6B). Staining with gold-labeled *anti*-biotin antibodies followed by TEM also confirmed that the particles were labeled with biotin (Fig. 6C).

Addressability of carboxyl groups

Next we attempted to label exposed carboxyl groups with biotin, first by priming with EDC to produce the active intermediate *O*-acylisourea ester. The amine group of biotin hydrazide can then attack this intermediate to form an amide bond (Fig. 7). Biotin conjugation was confirmed by western blot, SEC and TEM as described above (Fig. 6).

Discussion

VNPs are suitable for a vast range of applications ranging from medical imaging and drug delivery to the design of novel materials and electronic devices. It is important as part of the development process to determine the versatility of new VNPs and their tolerance of different chemical environments, particularly the harsh environments necessary for modification and functionalization. Many bioconjugation reactions must be carried out in the presence of the organic solvent DMSO, whereas ethanol is required for mineralization and electronic devices must be heat resistant. The tolerances are often highly constrained and specific, *e.g.* mineralization generally requires a narrow pH and temperature range specific for each mineral.[52] Novel SVPs such as the particles based on IBDV described herein must therefore undergo tolerance tests to study their integrity across a range of temperatures, pH values and solvent concentrations, and the accessibility of addressable conjugation targets on the particle surface must also be determined.

We expressed the IBDV major coat protein (VP2) in *Pichia pastoris* and, as previously reported,[44] isolated SVPs with a T = 1 surface lattice. We found that spectrophotometry was the most accurate method to determine particle concentration in solution because colorimetric methods cannot distinguish SVPs from stray peptides, whereas spectrophotometry generates separate peaks for peptides without aromatic side chains (190–220 nm) and proteins plus peptides with aromatic side chains (280 nm). We also analyzed particle integrity by NAGE, DLS and TEM.

DMSO is a versatile solvent for bioconjugation but high concentrations can induce conformational changes in proteins by binding to hydrophobic and aromatic side chains that are normally shielded inside the structure, resulting in precipitation.[53] Similarly, ethanol is required for mineralization reactions but high concentrations disrupt intramolecular hydrogen bonds and cause proteins to denature and precipitate.[54] We found that IBD-SVPs remained stable in solutions containing up to 20% (v/v) DMSO or ethanol, but that higher concentrations altered the electrophoretic mobility of the particles and caused them to precipitate. DLS showed that particles in 20% (v/v) ethanol and DMSO increased in size (the radius increased by 1.3 and 0.6 nm, respectively; Fig. 2C). In contrast, 50% (v/v) DMSO either stretched the particle into an elliptical conformation or compacted them to a

smaller radius (peak at 10 nm as determined by DLS, Fig. 2C) which induced rapid precipitation and resulted in higher electrophoretic mobility.

Previous studies have shown that IBDV is moderately stable in an acidic environment (pH 3), and also in the presence of certain disinfectants and when heated to 60 °C for 30 min.[55] We expected the corresponding SVP to have similar properties despite the additional rigidity of the parent virus conferred by RNA–protein and heteromeric protein–protein interactions, because the VP2 protein plays an important role in virion stability. We found that the IBD-SVPs were thermostable at 60 °C for 1 h, retaining 90% of the solubility observed at room temperature (Fig. 3B). After incubation at 68 °C for 1 h, 70% of the particles remained stable and soluble. VLPs can display extraordinary thermostability, *e.g.* bacteriophage PP7 VLPs are stable at 90 °C for more than 2 min because of the disulfide bonds linking coat protein dimers.[56] IBD-SVPs do not form disulfide bonds but strong interactions between VP2 momomers help to preserve the integrity of the particles at temperatures between 60 and 70 °C, making their heat tolerance comparable to CPMV.[51]

The IBD-SVPs were also stable across a wide pH range. As previously reported,[37] TEM analysis revealed minor conformational changes—particles were more condensed at pH 9.0—in alkaline solutions but this did not affect the hydrodynamic radius of the particles, and the slight change in electrophoretic mobility is likely to reflect the differing net charge of the particles in different pH environments. The IBD-SVPs therefore appear comparable to acidophilic viruses such as *Sulfolobus islandicus* rod shaped virus 2 (isolated from pH 2.5 acidic springs in Iceland).[5]

The ability to modify specific sites on the surface of VNPs allows them to be used as scaffolds that can be functionalized with diverse reagents including peptides, nucleic acids, metal ions, organic molecules and fluorescent dyes. Amine groups on lysine side chains are often used as attachment sites, *e.g.* for polymers,[57] fluorescent dyes[6,13] and redox-active complexes.[58] There are five accessible lysine side chains per VP2 monomer, and with each SVP comprising 60 VP2 subunits this equates to 300 accessible amine groups per particle. Carboxyl groups on the side chains of acidic residues can also be used as attachment sides following activation, if the conjugation target contains a primary amine group.[13,59,60] Each VP2 monomer has four Glu residues and nine Asp residues with an accessible carboxyl group, making 13 accessible sites per monomer and potentially 780 per SVP. TEM analysis confirmed successful biotinylation; several antibodies were bound per IBD-SVP (Fig. 6B), indicating multivalent display of biotin moieties. The immunostaining and TEM method, however, can not be regarded as a quantitative method; steric hindrance effects prevent large numbers of gold-labeled *anti*-biotin antibodies binding to the SVP surface.[5] To gain quantitative data on biotin labeling efficiency, we determined the number of addressable amine sites per SVP by the direct coupling of fluorescent (Alexa fluor 488) *N*-hydroxysuccinimide (NHS) esters. This showed that each SVP carried an average of 60 dye molecules, indicating that only one amine side chain can be occupied on each monomer, perhaps due to steric hindrance of the four remaining lysine residues once the first dye molecule is installed.

We observed a small amount of inter-particle aggregation during carboxylate conjugation, probably reflecting the formation of peptide bonds between the activated carboxyl groups on one particle and exposed amine groups on the lysine side chains of other particles (data not shown), but overall the integrity of the particles was maintained with both conjugation methods. It has previously been suggested that the sensitivity of IBD-SVP detection by spectrophotometry (A280) is too low for SEC.[61] We found that A215 measurements are more useful for this purpose and show adequate sensitivity.

Conclusions

The IBDV major coat protein (VP2) was expressed successfully in the yeast *Pichia pastoris* yielding large quantities of subviral particles (IBD-SVPs). We have established a simple and rapid procedure for the production of IBD-SVPs with high purity, and these were shown to be stable in 20% (v/v) solutions of DMSO or ethanol and also resistant to heat and pH extremes. This means IBD-SVPs can be used under the harsh environmental conditions required for bioconjugation, mineralization and other modifications. For the first time, we have demonstrated that IBD-SVPs can be functionalized on exposed amine and carboxyl groups by decorating the particles with biotin. The combination of stability, accessibility and amenability for large-scale production in yeast makes IBD-SVPs a potential platform for diverse applications in nanobiotechnology. The multivalent display of fluorescent molecules at discrete sites on the VNP surface could provide a high density of such traceable molecules without fluorescent quenching, increasing the sensitivity of detection. Combined with the possibility of dual labeling, IBD-SVPs could also be developed as a multifunctional platform, *e.g.* carrying both targeting ligands and fluorescent tracers for bioimaging applications.[62,63] IBD-SVPs could therefore be developed as a novel platform for medical imaging and/or targeted drug delivery.

Acknowledgments

We thank Dr Jörg Bornemann (Uniklinikum, RWTH Aachen University) for help with electron microscopy and Dr Thomas Eckert (Institute of Physical Chemistry, RWTH Aachen University) for help with DLS analysis. We acknowledge funding from the German Academic Exchange Service (DAAD) to OT and from NIH/NIBIB (R00 EB009105) to NFS. We also acknowledge Dr Richard M Twyman for revision of the manuscript.

References

1. Singh P, Prasuhn D, Yeh RM, Destito G, Rae CS, Osborn K, Finn MG, Manchester M. J. Controlled Release. 2007; 120:41.
2. Steinmetz NF, Evans DJ. Org. Biomol. Chem. 2007; 5:2891. [PubMed: 17728853]
3. Destito G, Yeh R, Rae CS, Finn MG, Manchester M. Chem. Biol. 2007; 14:1152. [PubMed: 17961827]
4. Steinmetz NF, Shah SN, Barclay JE, Rallapalli G, Lomonossoff GP, Evans DJ. Small. 2009; 5:813. [PubMed: 19197969]
5. Steinmetz NF, Bize A, Findlay KC, Lomonossoff GP, Manchester M, Evans DJ, Prangishvili D. Adv. Funct. Mater. 2008; 18:3478.
6. Steinmetz NF, Mertens ME, Taurog RE, Johnson JE, Commandeur U, Fischer R, Manchester M. Nano Lett. 2010; 10:305. [PubMed: 20017489]
7. Lee LA, Niu Z, Wang Q. Nano Res. 2009; 2:349.
8. Bronstein LM. Small. 2011; 7:1609. [PubMed: 21520496]

9. Grasso S, Santi L. Int J Physiol Pathophysiol Pharmacol. 2010; 2:161. [PubMed: 21383892]
10. Rae CS, Khor IW, Wang Q, Destito G, Gonzalez MJ, Singh P, Thomas DM, Estrada MN, Powell E, Finn MG, Manchester M. Virology. 2005; 343:224. [PubMed: 16185741]
11. McCormick AA, Palmer KE. Expert Rev. Vaccines. 2008; 7:33. [PubMed: 18251692]
12. Nichols ME, Stanislaus T, Keshavarz-Moore E, Young HA. J. Biotechnol. 2002; 92:229. [PubMed: 11689247]
13. Barnhill HN, Reuther R, Ferguson PL, Dreher T, Wang Q. Bioconjugate Chem. 2007; 18:852.
14. Wang Q, Kaltgrad E, Lin T, Johnson JE, Finn MG. Chem. Biol. 2002; 9:805. [PubMed: 12144924]
15. Wang Q, Lin T, Johnson JE, Finn MG. Chem. Biol. 2002; 9:813. [PubMed: 12144925]
16. Wang Q, Lin T, Tang L, Johnson JE, Finn MG. Angew. Chem., Int. Ed. 2002; 41:459.
17. Wang Q, Raja KS, Janda KD, Lin T, Finn MG. Bioconjugate Chem. 2003; 14:38.
18. Raja KS, Wang Q, Finn MG. Chem Bio Chem. 2003; 4:1348.
19. Gillitzer E, Willits D, Young M, Douglas T. Chem. Commun. 2002:2390.
20. Barnhill HN, Claudel-Gillet S, Ziessel R, Charbonniere LJ, Wang Q. J. Am. Chem. Soc. 2007; 129:7799. [PubMed: 17542581]
21. Schlick TL, Ding Z, Kovacs EW, Francis MB. J. Am. Chem. Soc. 2005; 127:3718. [PubMed: 15771505]
22. Miermont A, Barnhill H, Strable E, Lu X, Wall KA, Wang Q, Finn MG, Huang X. Chem.–Eur. J. 2008; 14:4939. [PubMed: 18431733]
23. Kaltgrad E, O'Reilly MK, Liao L, Han S, Paulson JC, Finn MG. J. Am. Chem. Soc. 2008; 130:4578. [PubMed: 18341338]
24. Sapsford KE, Soto CM, Blum AS, Chatterji A, Lin T, Johnson JE, Ligler FS, Ratna BR. Biosens. Bioelectron. 2006; 21:1668. [PubMed: 16216488]
25. Destito G, Yeh R, Rae CS, Finn MG, Manchester M. Chem. Biol. 2007; 14:1152. [PubMed: 17961827]
26. Mason HS, Lam DM, Arntzen CJ. Proc. Natl. Acad. Sci. U. S. A. 1992; 89:11745. [PubMed: 1465391]
27. Remond M, Da Costa B, Riffault S, Parida S, Breard E, Lebreton F, Zientara S, Delmas B. Vaccine. 2009; 27:93. [PubMed: 18983883]
28. Tsoka S, Ciniawskyj OC, Thomas OR, Titchener-Hooker NJ, Hoare M. Biotechnol. Prog. 2000; 16:661. [PubMed: 10933843]
29. Brumfield S, Willits D, Tang L, Johnson JE, Douglas T, Young M, Gen J. Virol. 2004; 85:1049.
30. Allnutt FC, Bowers RM, Rowe CG, Vakharia VN, LaPatra SE, Dhar AK. Vaccine. 2007; 25:4880. [PubMed: 17524532]
31. Brown SD, Fiedler JD, Finn MG. Biochemistry. 2009; 48:11155. [PubMed: 19848414]
32. Manzenrieder F, Luxenhofer R, Retzlaff M, Jordan R, Finn MG. Angew. Chem. Int. Ed. Engl. 2011; 50:2601. [PubMed: 21370346]
33. Yamada T, Iwasaki Y, Tada H, Iwabuki H, Chuah MK, VandenDriessche T, Fukuda H, Kondo A, Ueda M, Seno M, Tanizawa K, Kuroda S. Nat. Biotechnol. 2003; 21:885. [PubMed: 12833071]
34. Caston JR, Martinez-Torrecuadrada JL, Maraver A, Lombardo E, Rodriguez JF, Casal JI, Carrascosa JL. J. Virol. 2001; 75:10815. [PubMed: 11602723]
35. Dhar AK, Bowers RM, Rowe CG, Allnutt FC. Antiviral Res. 2010; 85:525. [PubMed: 20060858]
36. Shah SN, Steinmetz NF, Aljabali AA, Lomonossoff GP, Evans DJ. Dalton Trans. 2009:8479. [PubMed: 19809720]
37. Reiss BD, Mao C, Solis DJ, Ryan KS, Thomson T, Belcher AM. Nano Lett. 2004; 4:1127.
38. Steinmetz NF, Evans DJ, Lomonossoff GP. Chembiochem. 2007; 8:1131. [PubMed: 17526061]
39. Peabody DS. J. Nanobiotechnology. 2003; 1:5. [PubMed: 12890286]
40. Strable E, Prasuhn DE Jr, Udit AK, Brown S, Link AJ, Ngo JT, Lander G, Quispe J, Potter CS, Carragher B, Tirrell DA, Finn MG. Bioconjug. Chem. 2008; 19:866. [PubMed: 18318461]
41. Dey S, Upadhyay C, Madhan Mohan C, Kataria JM, Vakharia VN, Virol J. Methods. 2009; 157:84.

42. Saugar I, Luque D, Ona A, Rodriguez JF, Carrascosa JL, Trus BL, Caston JR. Structure. 2005; 13:1007. [PubMed: 16004873]
43. Garriga D, Querol-Audi J, Abaitua F, Saugar I, Pous J, Verdaguer N, Caston JR, Rodriguez JF. J. Virol. 2006; 80:6895. [PubMed: 16809295]
44. Lee CC, Ko TP, Chou CC, Yoshimura M, Doong SR, Wang MY, Wang AH. J. Struct. Biol. 2006; 155:74. [PubMed: 16677827]
45. Hermanson, GT. Bioconjugate techniques. Elsevier: London: Academic press; 1996.
46. Shamsara M, Ghorashi SA, Ahmadian G. Acta Virol. 2006; 50:229. [PubMed: 17177607]
47. Wu S, Letchworth GJ. Biotechniques. 2004; 36:152. [PubMed: 14740498]
48. Kim R, Yokota H, Kim SH. Anal. Biochem. 2000; 282:147. [PubMed: 10860512]
49. Provencher S. Comput. Phys. Commun. 1982; 27:229.
50. Provencher SW. Comp. Phys. Commun. 1982; 27:213.
51. Strable E, Finn MG. Curr. Top Microbiol. Immunol. 2009; 327:1. [PubMed: 19198568]
52. Douglas T, Shenton W, Young M, Stubbs G, Mann S. Adv. Mater. 1999; 3:253.
53. Arakawa T, Kita Y, Timasheff SN. Biophys. Chem. 2007; 131:62. [PubMed: 17904724]
54. Falk K, Lau JM, Santambrogio L, Esteban VM, Puentes F, Rotzschke O, Strominger JL, Biol J. Chem. 2002; 277:2709.
55. MacLachlat, JL., Stott, NJ. Veterinary microbiology. 2nd. Hirsh, DC.MacLachlan, NJ., Walker, RL., editors. Vol. Ch. 64. Ames, Iowa: Blackwell Publishing; 2005. p. 407-409.
56. Caldeira JC, Peabody DS. J. Nanobiotechnology. 2007; 5:10. [PubMed: 18039380]
57. Comellas-Aragones M, de la Escosura A, Dirks AT, van derHam A, Fuste-Cune A, Cornelissen JJ, Nolte RJ. Biomacromolecules. 2009; 10:3141. [PubMed: 19839603]
58. Steinmetz NF, Lomonossoff GP, Evans DJ. Small. 2006; 2:530. [PubMed: 17193081]
59. Steinmetz NF, Lomonossoff GP, Evans DJ. Langmuir. 2006; 22:3488. [PubMed: 16584217]
60. Schlick TL, Ding Z, Kovacs EW, Francis MB. J. Am. Chem. Soc. 2005; 127:3718. [PubMed: 15771505]
61. Cheng YS, Lee MS, Lai SY, Doong SR, Wang MY. Biotechnol. Prog. 2001; 17:318. [PubMed: 11312710]
62. Brunel FM, Lewis JD, Destito G, Steinmetz NF, Manchester M, Stuhlmann H, Dawson PE. Nano Lett. 2010; 10:1093. [PubMed: 20163184]
63. Lockney DM, Guenther RN, Loo L, Overton W, Antonelli R, Clark J, Hu M, Luft C, Lommel SA, Franzen S. Bioconjugate Chem. 2011; 22:67.

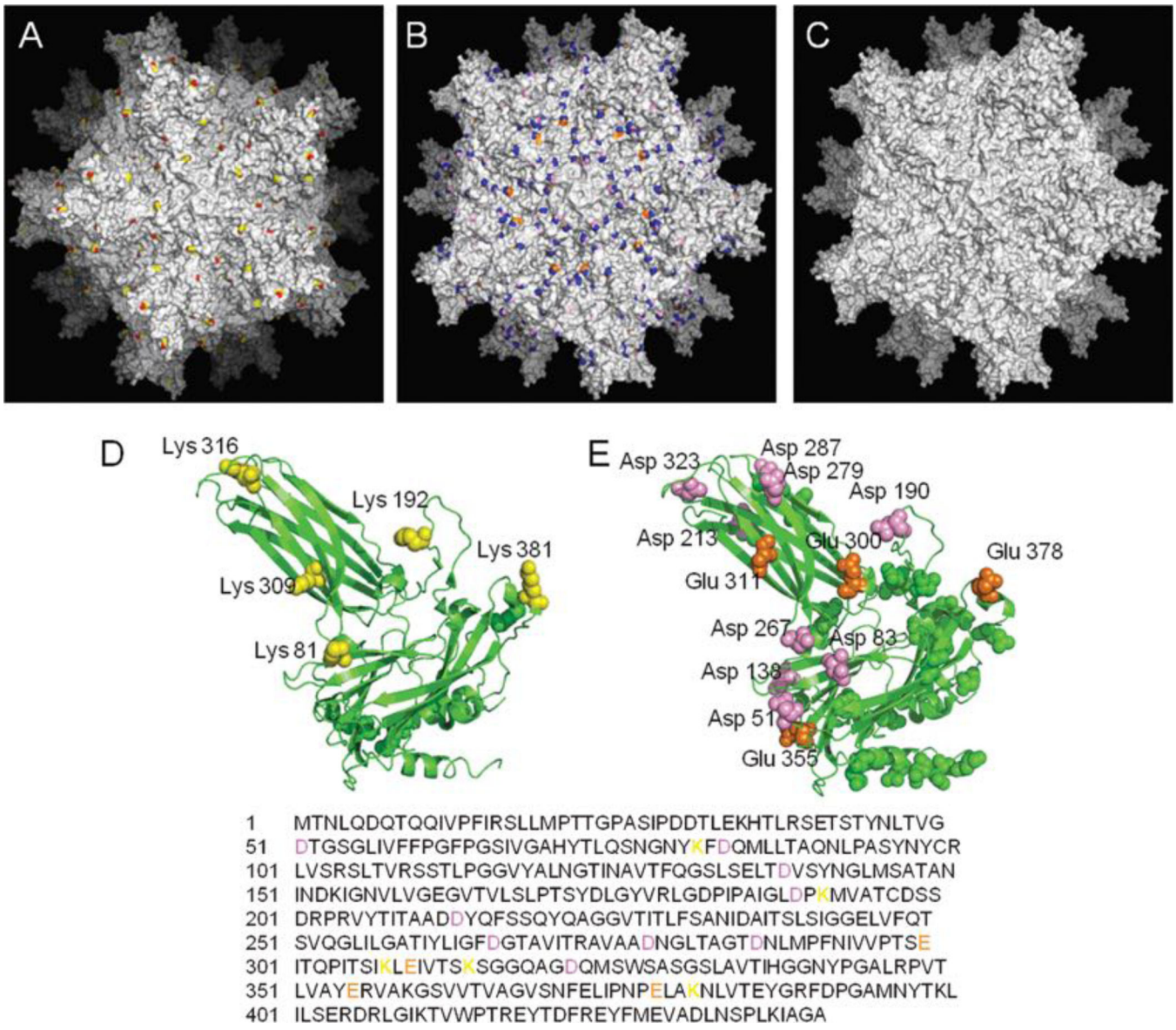

Fig. 1.

Structural analysis of IBD-SVPs. (A) Surface Lys residues shown in yellow and reactive amine side chains highlighted in red. (B) Surface Glu and Asp residues shown in orange and pink, respectively. The reactive carboxyl side chains of both residues are highlighted in blue. (C) Surface Cys residues are shown in purple, but the potentially reactive thiol groups are hidden inside and not exposed to the solvent. (D) The IBD-SVP asymmetric unit (VP2) is shown in green with five solvent-exposed amine residues in yellow. (E) Nine and four solvent-exposed Glu and Asp residues rendered in orange and pink respectively. All the figures of protein coordinates were rendered using the program PyMOL using the file with PDB code 2DF7.[44]

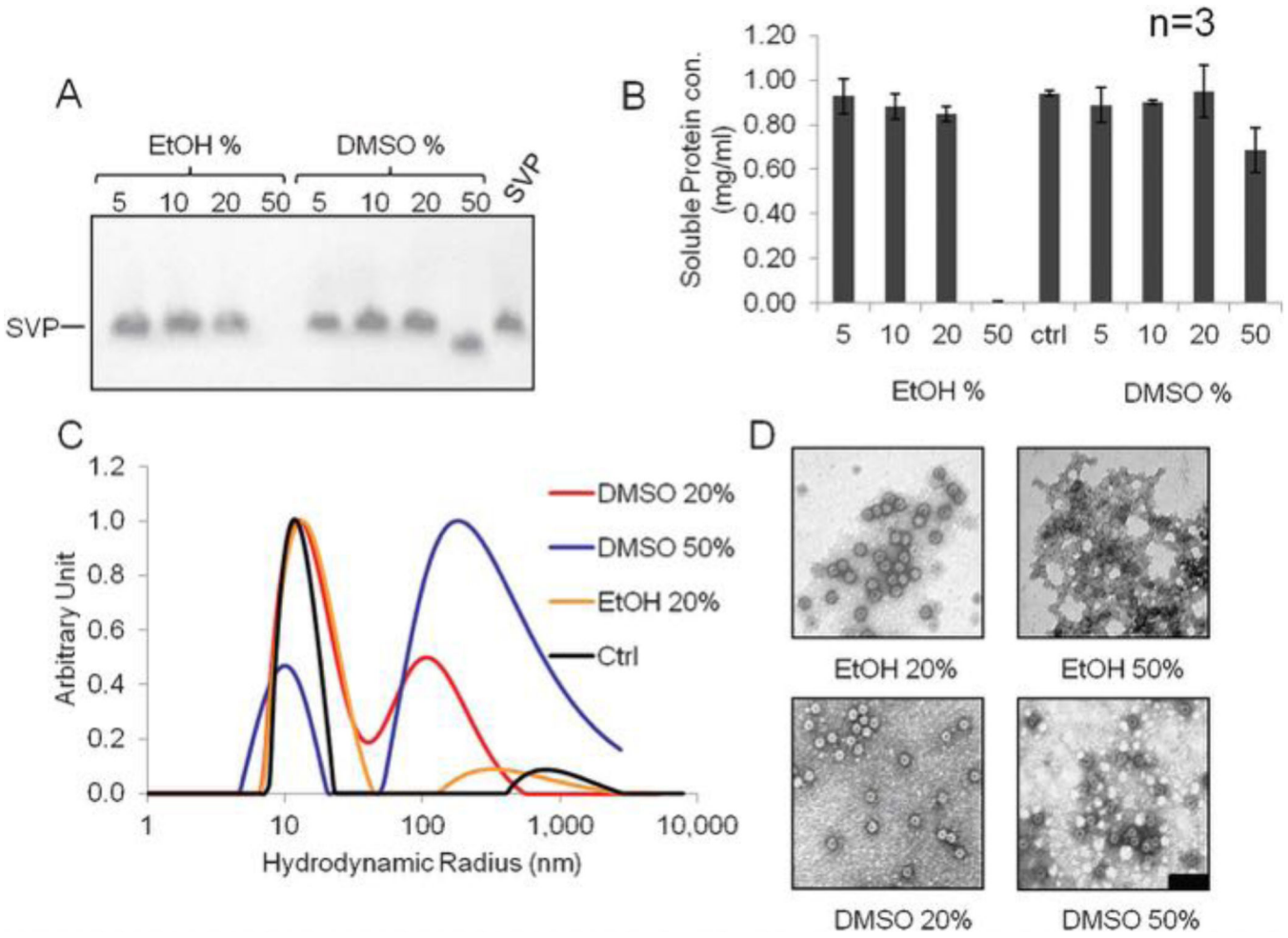

Fig. 2.

Stability of IBD-SVPs in ethanol–water and DMSO–water mixtures determined by NAGE (A), A280 spectroscopy (B), DLS (C) and TEM (D). Particles were dissolved in 5, 10, 20 and 50% (v/v) ethanol–water and DMSO–water, respectively. After 24 h the samples centrifuged at 13 000 × g for 20 min and the supernatant was analyzed. All the protein precipitated in 50% ethanol so in this case the pellet was used for TEM. Scale bar = 100 nm. As a control (ctrl), SVPs were dissolved to the same concentration in PBS. Data shown in panel B are derived from three independent experiments; error bars show standard deviations.

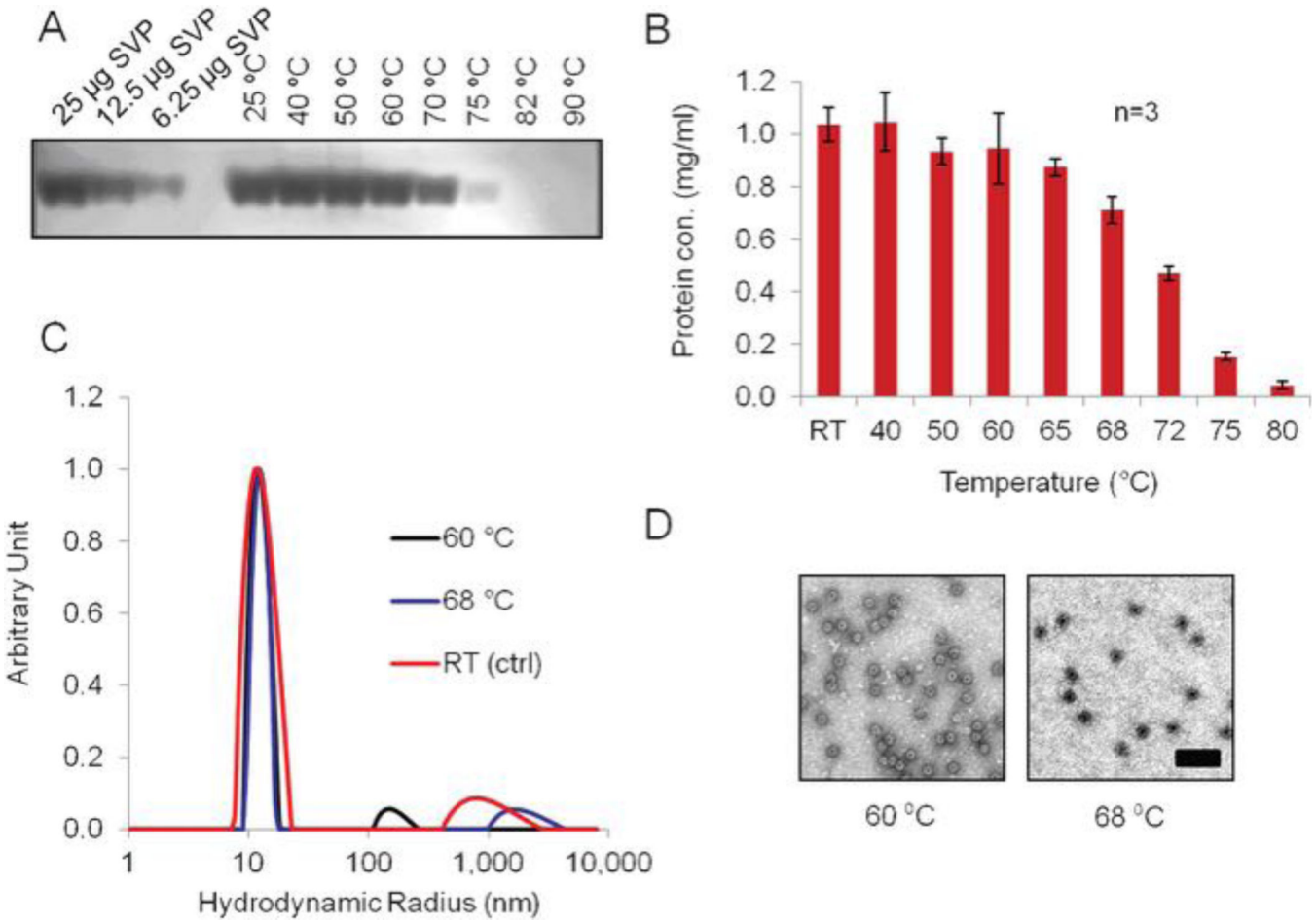

Fig. 3.

Stability of IBD-SVPs at different temperatures determined by NAGE (A), A280 spectroscopy (B), DLS (C) and TEM (D). SVPs were dissolved in PBS to a final concentration of 1 mg ml^{-1} and incubated for 1 h at 40, 50, 60, 65, 68, 72, 75 and 80 °C in a gradient thermocycler. The samples were then cooled on ice, centrifuged at 13 000 × g for 20 min at 4 °C, and the supernatant was used for analysis. Scale bar = 100 nm. SVPs incubated at room temperature were used as the control. Data shown in panel B are derived from three independent experiments; error bars show standard deviations.

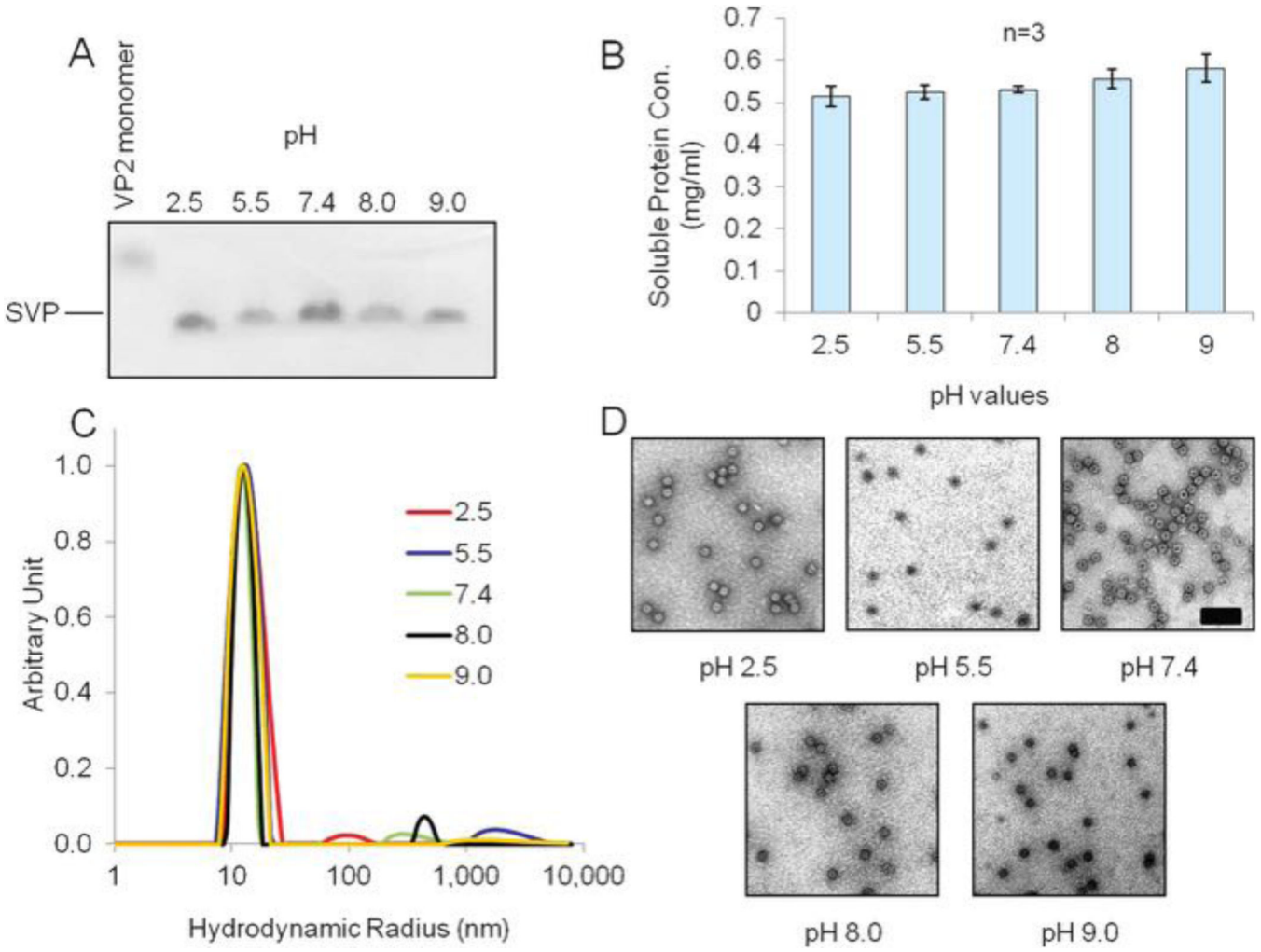

Fig. 4.

Stability of IBD-SVPs in different pH environments determined by NAGE (A), A280 spectroscopy (B), DLS (C) and TEM (D). Particles were dissolved in buffers at pH 2.5, 5.5, 7.4, 8.0 and 9.0, to final concentration of ~0.5 mg ml^{-1}. The samples were incubated overnight at room temperature and centrifuged at 13 000 × g for 20 min at 4 °C, and the supernatant was used for analysis. Scale bar = 100 nm. SVPs incubated at pH 7.4 were used as the control. Data shown in panel B are derived from three independent experiments; error bars show standard deviations.

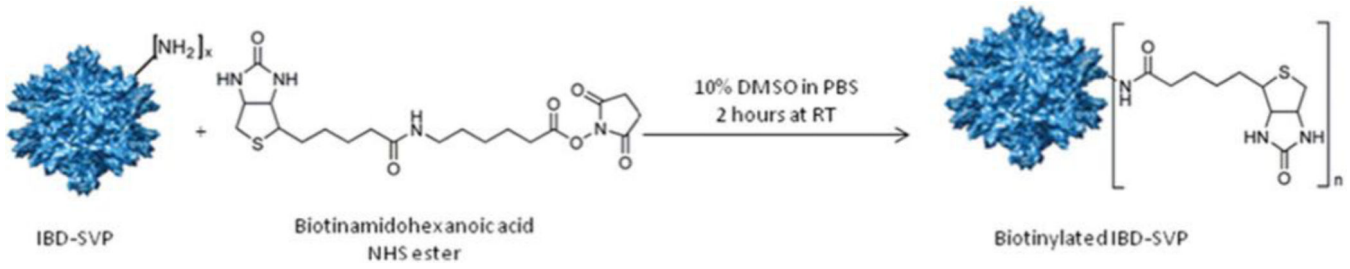

Fig. 5.

Labeling of amine groups on the surface of IBD-SVPs using biotinamidohexanoic acid *N*-hydroxysuccinimide ester. Schematic IBD-SVP refers to Protein Data Bank reference 2DF7.[20] Purple circles represent biotin.

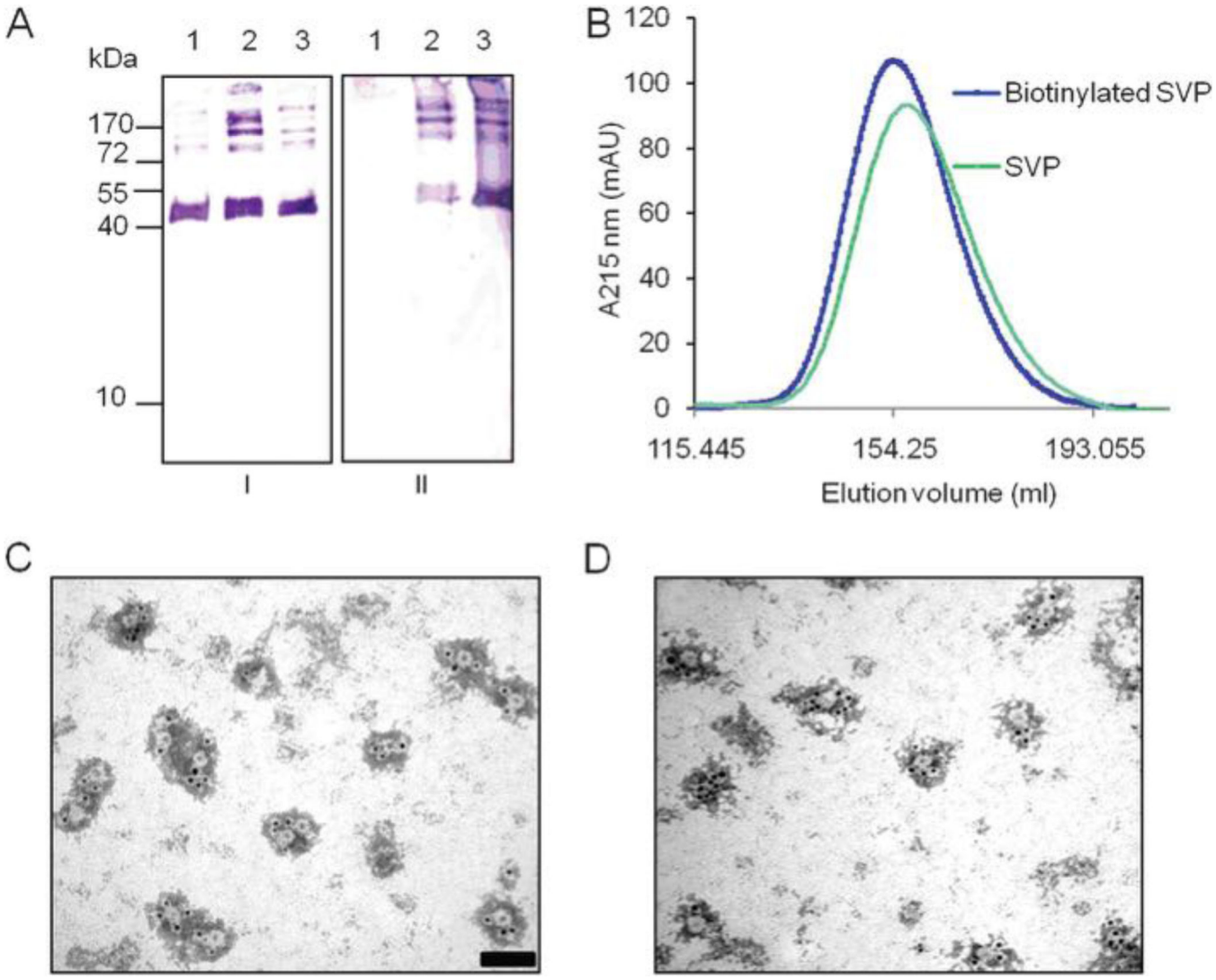

Fig. 6.

Biochemical analysis of biotinylated IBD-SVPs by western blot (A), SEC (B), TEM after amine conjugation (C) and TEM after carboxyl conjugation (D). Western blot was performed either by subsequent incubation with rabbit *anti*-IBD-VP2 (1 : 10 000) and phosphatase-conjugated goat *anti*-rabbit antibody (final concentration 2 μg ml^{-1}) each for 1 h at room temperature (AI) or by incubating with alkaline phosphatase-conjugated streptavidin (final concentration 0.2 μg ml^{-1} in PBS) for 1 h at room temperature (AII). The signal was detected with NBT/BCIP (Sigma); IBD-SVPs (lane 1), biotinylated IBD-SVPs *via* amine and carboxyl chemistry (lane 2 and 3 respectively) were analyzed. SEC was carried out using a Hiprep 26/60 Sephacryl S400 column and Äkta Explorer. Samples were analyzed at a flow rate of 0.5 ml min^{-1}, and elution profiles were detected by spectrophotometry (A215). TEM micrographs show biotinylated SVPs detected with a gold-labeled goat *anti*-biotin antibody (1 : 20 in PBS). Scale bar = 50 nm.

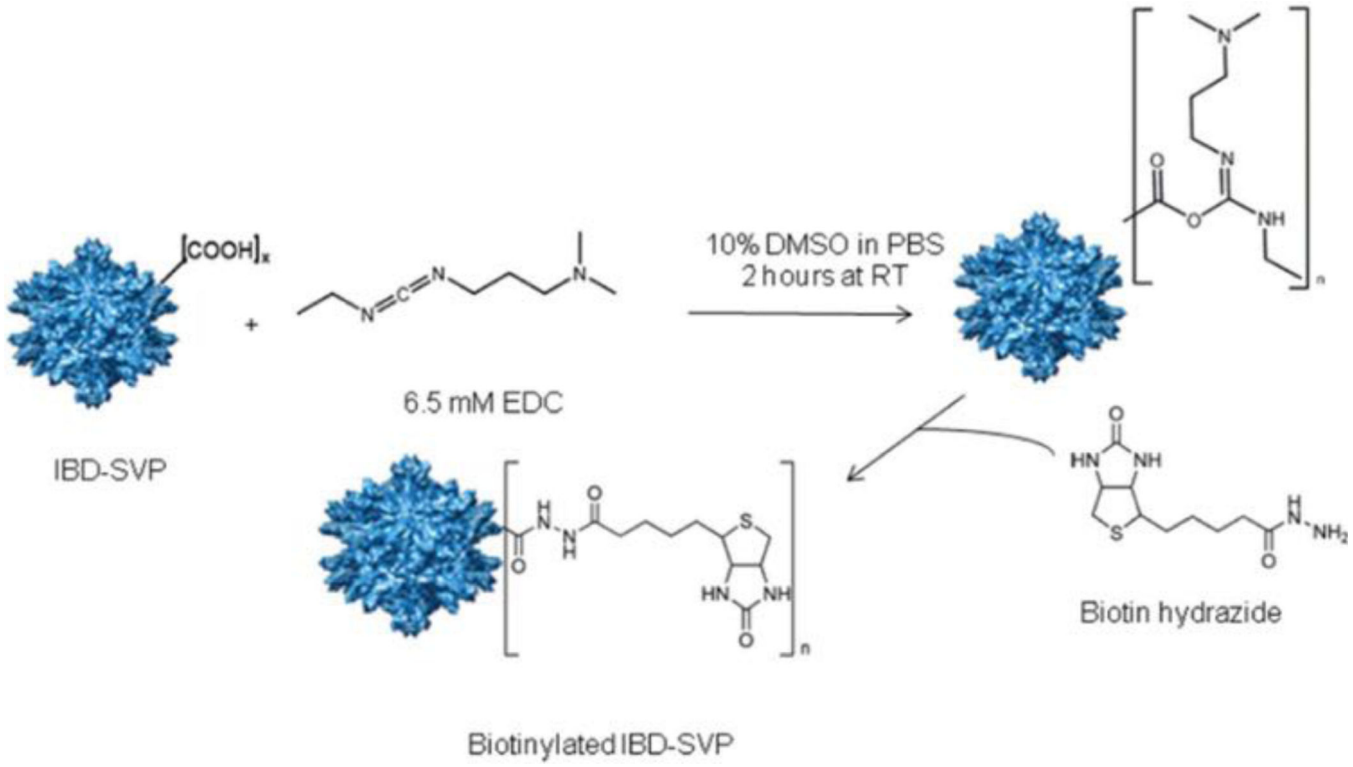

Fig. 7.

Labeling carboxyl groups on the surface of IBD-SVP. Reaction with EDC (1-[3-(dimethylamino)propyl]-3ethylcarbodiimide methiodide) produces the intermediate *O*-acylisourea which reacts with the amine group of biotin hydrazide. Schematic IBD-SVP refers to Protein Data Bank reference 2DF7.[20] Purple circles represent biotin.